STATIC PRESSURE CONTROL FOR BALANCING VAV SYSTEMS AND MINIMIZING ENERGY CONSUMPTION: A COMPUTER SIMULATION STUDY

M. Zaheer-uddin and G.R. Zheng
Centre for Building Studies
Concordia University
1455 de Maisonneuve Blvd. West
Montreal, Que. Canada H3G 1M8

ABSTRACT

A transient model of a two-zone variable air volume (VAV) system is developed. The system consists of two environmental zones, a cooling and dehumidifying coil, fan and ductwork, chiller and a storage tank. Results showing the transient response of the open-loop system are given. The use of speed control as a means of balancing the static pressure in the ductwork and minimizing fan energy consumption is illustrated.

INTRODUCTION

Although Variable Air Volume (VAV) systems have been found to be energy efficient, they are also known to be difficult to control [1]. The reason for this is that when zone dampers are modulated in response to feedback from the zone thermostat, the static pressure in the ductwork is affected. This causes what is known as off-balance problem in VAV systems. At low loads, the zone dampers modulate towards some minimum position. As a consequence the pressure drop across the dampers will increase. If no control action is taken to deal with this situation, the fan discharge pressure will increase causing excessive use of energy. In most practical systems, some volume control at the fan inlet is provided. Another approach often used is fan speed control. In either case the feedback signal must come from a static pressure sensor located in the duct system.

Despite the fact that static pressure control is used in practical VAV systems, problems do exist such as less than marginal energy savings and improper air flow rates to the zones. Furthermore, the use of proper quantities of outdoor air for maintaining acceptable indoor air quality via damper control adds another dimension to the control of VAV systems. For an optimum operation of VAV system, a balance between the zone loads, the air flow rate in the ducts and the fan power must be achieved. In order to study this balancing act, a comprehensive time dependant model of a multizone VAV system must be developed. In this paper we develop a transient model of a multizone VAV system and study the response characteristics of zone temperatures, humidity ratios, static pressure and the fan power subject to step changes in cooling loads.

We note that both experimental and theoretical studies have been done on VAV systems [2-4]. However the majority of these studies consider only specific issues. A comprehensive model of a multizone VAV system is required for designing good controllers which was the primary motivation for this study. The starting point for this study is the previous work [5] in which we have examined the closed-loop response of a single zone VAV system. We improve upon that study by extending it to multizone cases and furthermore consider the variable air flow rate in the duct system together with fan speed control. This increases the complexity of the model considerably which we think is necessary in order to simulate VAV systems realistically.

TRANSIENT MODEL OF A MULTIZONE VAV SYSTEM

Figure 1 shows the schematic diagram of a VAV system used in this study. The major elements of the system are: i) two environmental zones; ii) a cooling and dehumidifying coil; iii) a chiller and a storage tank; iv) a fan and v) duct work together with air flow control dampers at the zones, in the exhaust duct and the outdoor air intake duct. The face and bypass dampers are not yet included in the model at the present time.

The operation of the VAV system can be understood by tracing the path of return air around the loop. For example, the air from the zones return through the return duct, a portion of this air is exhausted and remaining air is mixed with the fresh outside air. The mixed air, which is hot and humid (considering the cooling case), is cooled and dehumidified in the cooling coil, which receives chilled water from the chiller and storage tank arrangement shown in the figure. The air leaving the coil must be at appropriate conditions (in terms of dry bulb temperature and humidity ratio) in order to satisfy the cooling load requirement of the zones. Therefore, for a good control of zone air temperatures and humidity ratios, the rate of supply air and to same degree its condition, must be continuously modulated.

As shown in the figure there are six control variables that can be varied in order to improve the overall response. For example, the outdoor air flow can be controlled by modulating the outdoor air dampers, the quantity of supply air is controlled by positioning the zone dampers and by controlling the fan speed. The condition of air leaving the coil is controlled by controlling the mass flow rate of chilled water flowing in the coil and also by controlling the temperature of chilled water entering the coil via chiller input energy control.

By using the mass, momentum and energy balance principles we have developed the governing equations of the system. These are

<u>Environmental zones</u>

$$V_{z,j} * \frac{\partial \rho_{zj}}{\partial t} = (\rho * V_a * A)_{s,j} - (\rho * V_a * A)_{r,j} \, , \tag{1}$$

$$C_p * V_{zj} \frac{d(\rho_{zj} * t_{zj})}{dt} = (\rho * V_a * A)_{s,j} * C_p * t_{sj} - (\rho * V_a * A)_{r,j} * C_p * t_{z,j} + Q_{s,j}(t) + Q_{l,j}(t) - l_g * \dot{m}_{w,j}(t) \, , \tag{2}$$

$$V_{zj} \frac{d(\rho_{zj} * W_{zj})}{dt} = (\rho * V_a * A)_{sj} * W_{s,j} - (\rho * V_a * A)_{rj} * W_{zj} + \dot{m}_{w,j}(t) \, , \tag{3}$$

for $j = 1, 2$

<u>Cooling and dehumidifying coil</u>

$$\gamma\frac{\partial(\rho*V_a*t_a)}{\partial y}+\frac{\partial(\rho*t_a)}{\partial t}+(1-\gamma)*t_a*\frac{\partial(\rho*W_a)}{\partial t}$$
$$=-\frac{h_c*\eta_{s,ov}*A_o}{c_vA}*(t_a-t_{t,o})-\frac{h_{l,d}*A_d}{c_vA}*(t_a-t_d) \tag{4}$$
$$+\frac{h_{m,c}*\eta_{c,ov}*A_o*C_w}{c_vA}*t_a*(W_a-W_{t,o,st})+\frac{h_{ml,d}*A_d*C_w}{c_vA}*t_a*(W_a-W_{d,st})$$

$$\frac{\partial(\rho*W_a)}{\partial t}+\frac{\partial(\rho*V_a*W_a)}{\partial y}=-\frac{h_{m,c}*\eta_{c,ov}*A_o}{A}*(W_a-W_{t,o,st})-\frac{h_{ml,d}*A_d}{A}*(W_a-W_{d,st}) \tag{5}$$

$$m_d*c_{pd}*\frac{\partial t_d}{\partial t}=h_{l,d}*A_d*(t_a-t_d)+h_{ml,d}*\lambda*A_d*(W_a-W_{d,st}) \tag{6}$$
$$+h_{e,d}*A_d*(t_\infty-t_d)+h_{me,d}*\lambda*A_d*(W_\infty-W_{d,st})$$

$$\frac{\partial\rho}{\partial t}+\frac{\partial(\rho*V_a)}{\partial y}=0 \tag{7}$$

$$\frac{\partial\rho}{\partial t}+\frac{\partial(\rho*V_a*V_a)}{\partial y}=-\frac{\partial P}{\partial y}-\frac{c_f*A_d}{2A}*\rho*V_a*V_a \tag{8}$$

$$\frac{\partial(\dot{m}_w*t_w)}{\partial x}+\frac{\partial(m_w*t_w)}{\partial t}=\frac{h_{l,c}*A_{tl}}{c_w}*(t_{t,o}-t_w) \tag{9}$$

$$\frac{\partial t_a}{\partial t}+\frac{\eta_s+\frac{m_t*C_t}{m_f*C_f}}{1-\eta_s}*\frac{\partial t_{t,o}}{\partial t}=\frac{\eta_{s,ov}*h_c*A_o}{m_f*c_f*(1-\eta_s)}*(t_a-t_{t,o}) \tag{10}$$
$$+\frac{\eta_{c,ov}*\lambda*h_{m,c}*A_o}{m_f*c_f*(1-\eta_s)}*(W_a-W_{t,o,st})-\frac{h_{l,c}*A_{tl}}{m_f*c_f*(1-\eta_s)}*(t_{t,o}-t_w)$$

$$P=\rho*R*T_a=\rho*R*(t_a+273.15) \tag{11}$$

Duct model

$$\gamma*\frac{\partial(\rho*V_a*t_a)}{\partial y}+\frac{\partial(\rho*t_a)}{\partial t}+(1-\gamma)*t_a*\frac{\partial(\rho*W_a)}{\partial t} \tag{12}$$
$$=-\frac{h_{l,d}*A_d}{c_vA}*(t_a-t_d)-\frac{h_{ml,d}*A_d*C_w}{c_vA}*t_a*(W_a-W_{d,st})$$

$$\frac{\partial(\rho*W_a)}{\partial t}+\frac{\partial(\rho*V_a*W_a)}{\partial y}=-\frac{h_{ml,d}*A_d}{A}*(W_a-W_{d,st}) \tag{13}$$

$$m_d*c_{pd}*\frac{\partial t_d}{\partial t}=h_{l,d}*A_d*(t_a-t_d)+h_{ml,d}*\lambda*A_d*(W_a-W_{d,st}) \tag{14}$$
$$+h_{e,d}*A_d*(t_\infty-t_d)+h_{me,d}*\lambda*A_d*(W_\infty-W_{d,st})$$

$$\frac{\partial\rho}{\partial t}+\frac{\partial(\rho*V_a)}{\partial y}=0 \tag{15}$$

$$\frac{\partial(\rho * V_a)}{\partial t} + \frac{\partial(\rho * V_a * V_a)}{\partial y} = -\frac{\partial P}{\partial y} - \frac{C_f}{2 * A} * \rho * V_a * V_a * A_d \tag{16}$$

$$P = \rho * R * T_a = \rho * R * (t_a + 273.15) \tag{17}$$

<u>Motor model</u>

$$J_{eq}\frac{dN}{dt} = \frac{k_t}{2\pi} * I - B_{eq} * N - \frac{Q \Delta P_f}{(2\pi)^2 * N * \eta_f} \tag{18}$$

$$L * \frac{dI}{dt} = e_a(t) - R * I - 2 * \pi * k_b * N \tag{19}$$

$$\textit{where} \qquad \Delta P_f = C_h * \rho_o * D^2 * N^2 * (\frac{n_m}{n_f})^2 \tag{20}$$

<u>Damper model</u>

$$\Delta P_d^j = \{ a_0 * EXP(a_1 * u^j) + a_2 \} * \frac{\rho_a V_a^2}{2} \qquad \text{for } j = 1, 2, ..., M \tag{21}$$

<u>Chiller and storage tank model</u>

$$C_{ws} * \frac{\partial t_{ws}}{\partial t} = - C_{p,w} \dot{m}_w \zeta * (t_{ws} - t_{wr}) - U_c * U_{s,max} * COP + U_{ch} A_{ch} (t_\infty - t_{ws}) \tag{22}$$

Because of the space limitations, we cannot give the nomenclature in detail. However, we note that the overall system model is nonlinear with variable parameters. The state variables of interest in the above equations are: zone temperatures (t_z); humidity ratios (W_z); density of air in the zones (ρ_z); describing the coil model we have temperature of air t_a, humidity ratio W_a, velocity of air flow V_a, temperature of chilled water t_w, tube temperature t_{to}, and duct temperature t_d; in the case of duct model we have similar set of state variables as in the coil model except without t_w, t_{to}; for the motor model we have speed N and motor current I; for the chiller model we have t_{ws} as the water temperature in the storage tank and P the coefficient of performance of the chiller.

The environmental zone model describes a balance between variable mass flow of air entering and leaving the zone (Eq.1), energy and moisture balance per Eqs.(2-3). The cooling and dehumidifying coil model describes heat and mass transfer occurring between variable flow of air and the cooling coil giving equations (4-11) for temperature t_a, humidity W_a of air and t_w for the temperature of chilled water in the coil. Equations (12-17) describes the duct model which consists of mass and momentum balance (Eqs.15-16) and the heat transfer with the surroundings (Plenum) (Eqs.12-14). In the case of motor model we have considered torque balance via Eq.(18) and time rate of changes in applied voltage Eq.(19). Equation (21) describes the pressure loss characteristics of typical dampers. Finally, the chiller model, Eq.(22) describes the energy balance between energy input to the chiller to withdraw heat from the water and the rate of heat added to the chilled water storage via the return water from the cooling coil. Thus, the overall model given by Eqs.(1-22) is coupled and nonlinear. We could examine the effect of several operating strategies with this model as described in the following section.

SIMULATION RESULTS

The governing equations were discretized in space and time and were solved using numerical integration methods with variable time step. A total of 270 equations were solved simultaneously at each time step. In the following we present the results showing the transient response of the open-loop system.

The simulated VAV system consisted of two zones with about 16.7 m^2 (180 ft^2) each in floor area. The cooling loads acting on the zones were: 4.2 kW sensible and 1.4 kW latent for zone 1; and 6.3 kW sensible and 2.1 kW latent for zone 2. The environmental zones were assumed to be about 100 meters away from the central system and therefore a total of approximately 300 m of ductwork is involved. A 8 row, 16 tube plate-fin-tube cooling and dehumidifying coil was simulated. The frontal area of the coil was 0.3716 m^2 (4 sqft). A fan with 2-HP motor was used. The fan was rated for a maximum static pressure of 500 Pa at 1200 rpm. A 20 kW chiller was used.

For the open-loop test, the zone dampers were kept full open. The outdoor air dampers were set at 20% open position. With the chiller and the fan full on, the time response characteristics of the VAV system were plotted (Figures 2a-2f). Figure 2a and 2b show the zone temperature and humidity ratio responses. It is apparent from Fig. 2a that approximately 20 minutes are needed for the zone temperatures to reach near steady state. The mass flow rates of supply and return air to and from each zones are depicted in Fig. 2c. Also shown in Figure 2c is the outdoor air flow rate response. For the system considered, a 20 % open dampers resulted in about 0.185 kg/s of outdoor air which turns out about 15% of the total air flow in the system. It may be noted that the air flow rates reach steady state rapidly in about 30 seconds. The response time is directly dependent on fan-motor characteristics. As shown in Fig. 2d the fan speed reaches steady state in about 30 seconds. The steady state speed of fan is about 1100 rpm. How the motor power varied during this time is shown in Figure 2e. The large overshoot is due to the start-up dynamics of the motor which are considerably faster than the zone temperature responses. Also shown in Fig. 2f are the static pressures at the fan outlet and also at a point approximately 2/3 of the distance from the coil. Normally, it is at this position a static pressure sensor is installed to control the air flow rates in the duct system. Taken together, figures 2a - 2f describe typical transient responses of the VAV system when subjected to step changes in the cooling loads on the zones. Ideally, we would like to automatically control the zone dampers, fan speed and chilled water mass flow rate in the coil in response to variable cooling loads acting on the zones. However, this requires design of controllers for VAV system which is presently being studied. Here we present some results of practical interest.

The zone temperatures can be controlled by modulating the zone dampers while holding the motor speed at nominal value (case 1) or by holding the dampers at certain fixed open position and controlling the fan speed (case 2). The case 2 is expected to result in energy savings compared to case 1. Furthermore, case 2 should be the preferred method of control as much as possible since it also provides a means of balancing the static pressure in the ductwork. To illustrate these ideas we present results from the simulation runs. Figure 3a - 3c show the results for each of the two cases cited above. For example, in order to reject a step change in cooling load of 2.52 kW sensible and 1.4 kW latent for zone 1; and 3.78 kW sensible and 2.1 kW latent for zone 2, how both cases achieved the zone temperature regulation is depicted in these figures. With supply air temperature remaining the same, both cases are able to bring the zone temperatures close to their respective setpoints (25±0.5 C) as shown in Fig. 3a. However, as depicted in Fig. 3b the motor power required in case 2 (114.7W) is only about 1/7 of the power required by the motor in case 1 (829.9W). This becomes apparent by noting that the static pressure which the fan must deliver in case 1 is much higher (since the dampers are partially closed) as shown in Fig. 3c. Thus, it is desirable to control the motor speed not only to save energy but also balance the static pressure to ensure proper air flow rates to the zones. For the example considered here, the magnitude of the static pressure which achieves the balance between cooling load and fan power is 101.35 kPa (case 2) shown in Fig.3c. In practice, this can be achieved by feedback signal from a static pressure sensor to control the fan speed. The design of such feedback controller is presently being studied.

CONCLUSIONS

A transient model of a two zone VAV system has been developed. The time response characteristics of the VAV system show that the steady state time for zone temperatures and humidity ratios is about 1200 seconds, and for the static pressure in the duct it is about 30 seconds. It has been shown that speed control can be used as means of balancing static pressure in the ductwork and minimizing fan energy consumption.

ACKNOWLEDGMENTS

This work was funded by grant (OGP 0036380) from the Natural Sciences and Engineering Research Council of Canada.

REFERENCES

[1] R.W. Haines, *Control systems for heating, ventilating and air conditioning,* Van Nostrand Reinhold Company, NY (1987)

[2] P.W. Brothers, and M.L. Warren, Fan energy use in variable air volume system, *ASHRAE Transactions*, Vol.92, Part 2B, pp.19-29, (1986)

[3] L.K. Norford, A. Rabl, and R.H. Socolow, Control of supply air temperature and outdoor air flow and its effect on energy use in variable air volume system, *ASHRAE Transactions*, Vol.92, Part 2B, pp.30-45, (1986)

[4] HVACSIM$^+$, *Building systems and equipment simulation program reference manual,* U.S. Department of Commerce, National Technical Information Service, (1986)

[5] M. Zaheer-uddin and P.A. Goh, Transient Response of a closed-loop VAV system, *ASHRAE Transactions*, Vol. 97, Part 2, (1991)

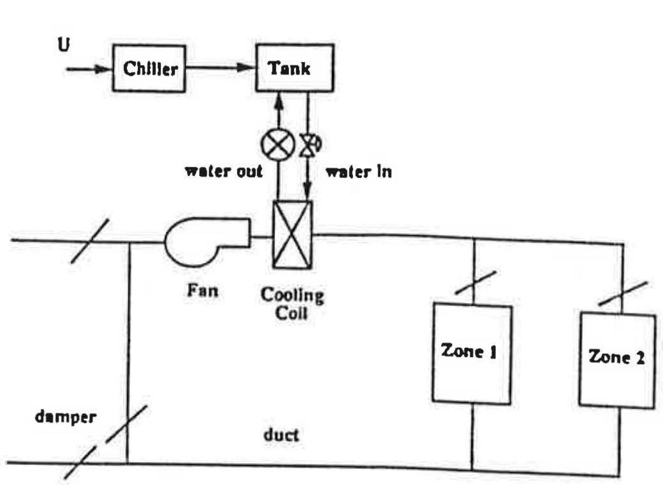

Figure 1. Schematic diagram of a VAV system

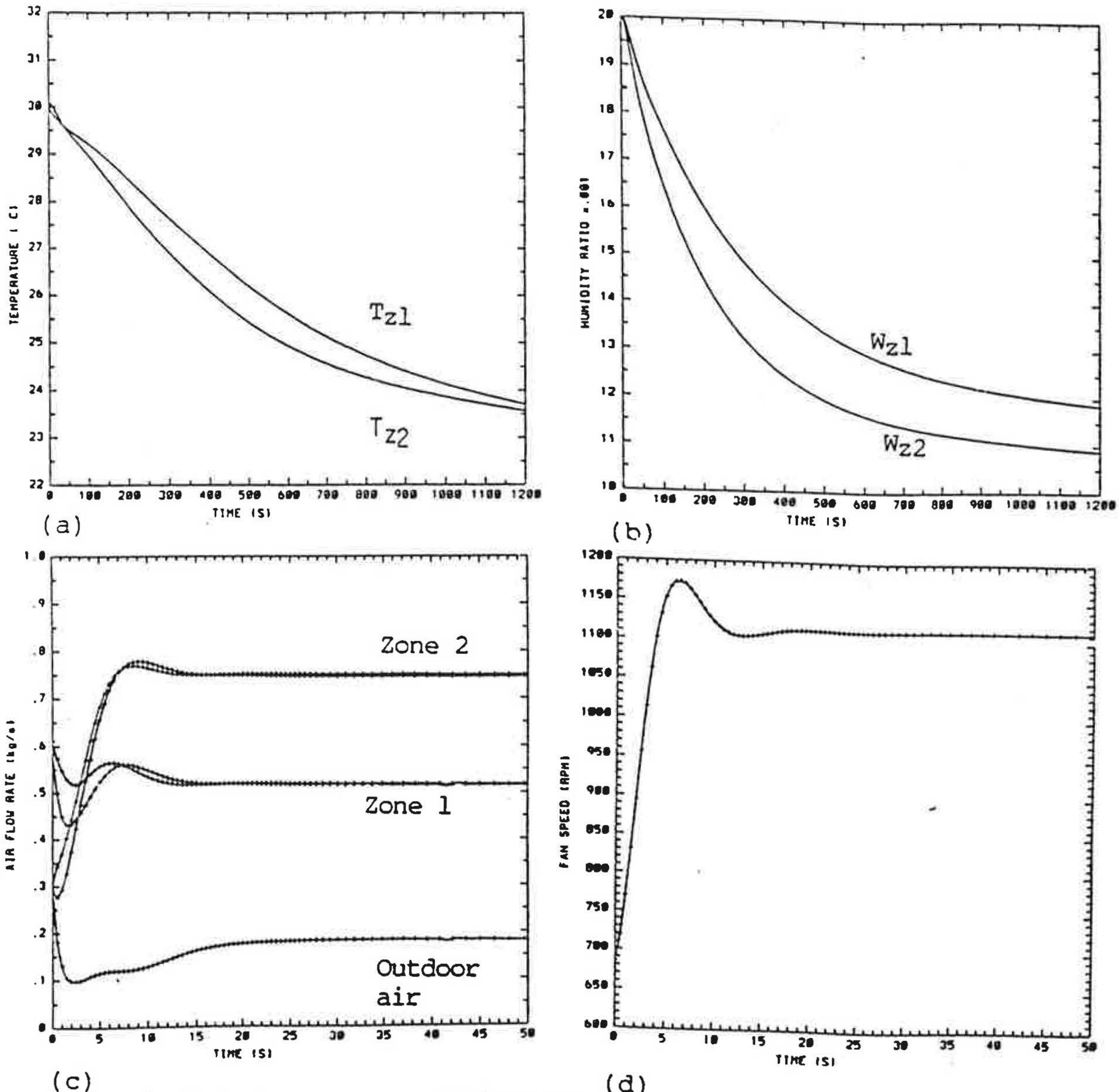

Figure 2. Output responses subject to a step change in cooling loads
(a) T_{z1}, T_{z2} responses (b) W_{z1}, W_{z2} responses
(c) Supply and outdoor air flow rates (d) Fan speed

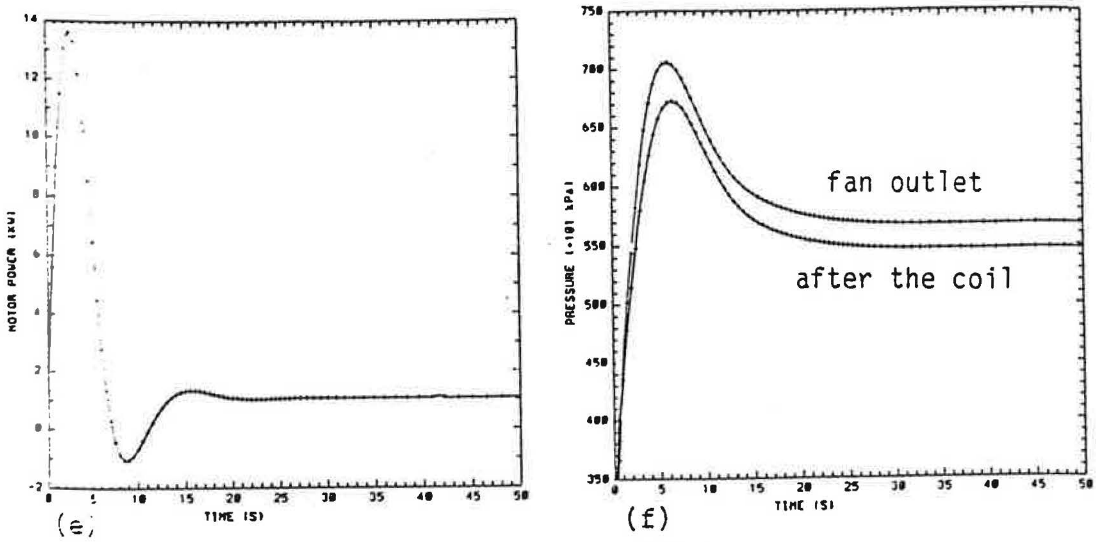

Figure 2 continued – (e) Motor power (f). Static pressure

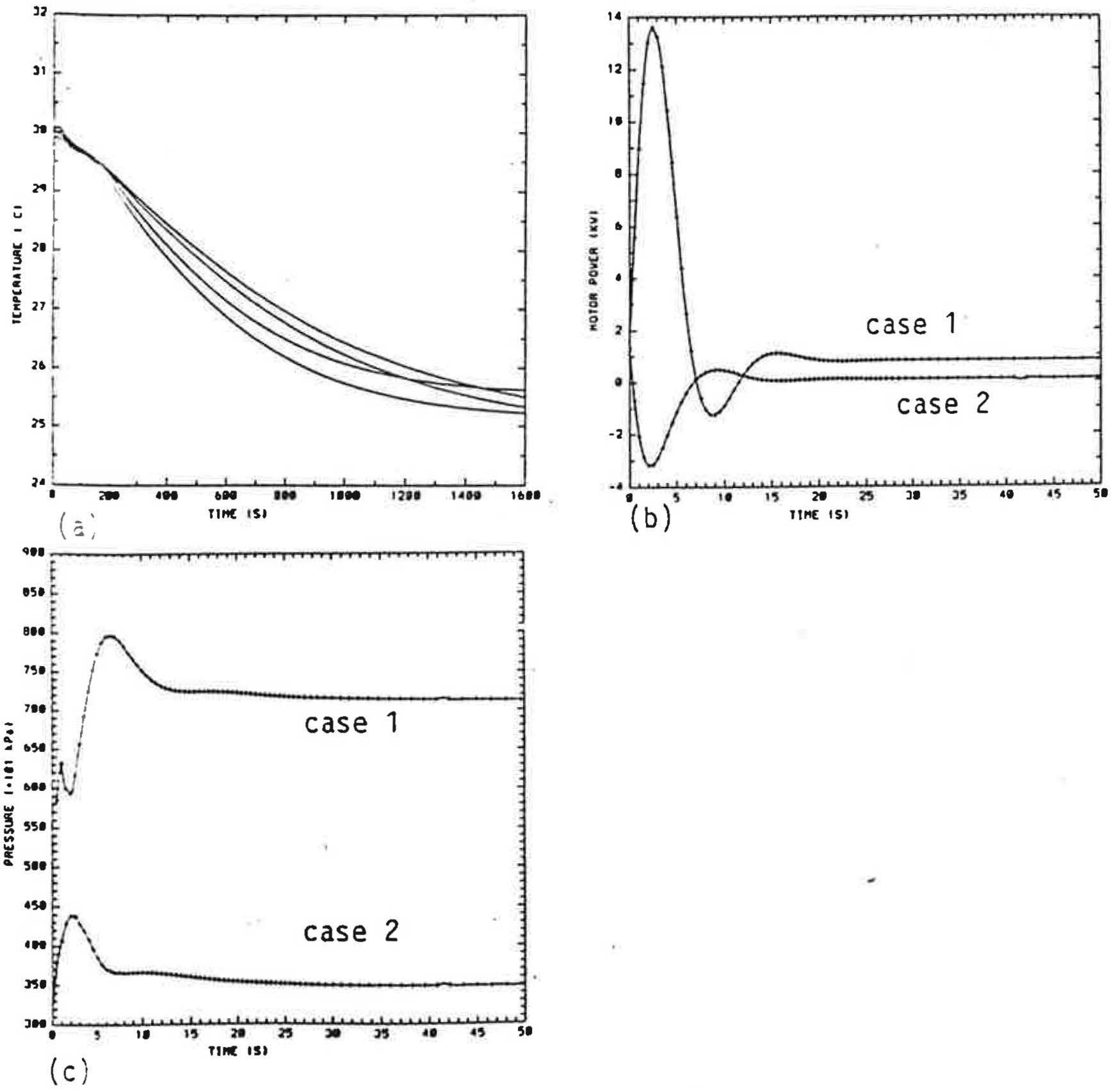

Figure 3. Simulation results from cases 1 and 2.
Case 1 - damper control, Case 2 - Speed control
(a). T_{z1}, T_{z2} for both cases
(b). Motor power (c). Static pressure